Ryo Kikuuwe
Machinery Dynamics Laboratory,
Hiroshima University,
1-4-1 Kagamiyama,
Higashi-Hiroshima, Hiroshima 739-8527, Japan
e-mail: kikuuwe@ieee.org

Tomofumi Okada
Kobelco Construction Machinery Dream-Driven
Co-Creation Research Center,
Hiroshima University,
1-4-1 Kagamiyama,
Higashi-Hiroshima, Hiroshima 739-8527, Japan

Hideo Yoshihara
Kobelco Construction Machinery Co., Ltd.,
2-2-1 Itsukaichiko,
Saeki-ku, Hiroshima 731-5161, Japan

Takayuki Doi
Kobelco Construction Machinery Co., Ltd.,
2-2-1 Itsukaichiko,
Saeki-ku, Hiroshima 731-5161, Japan

Takao Nanjo
Kobelco Construction Machinery Co., Ltd.,
2-2-1 Itsukaichiko,
Saeki-ku, Hiroshima 731-5161, Japan

Koji Yamashita
Kobelco Construction Machinery Co., Ltd.,
2-2-1 Itsukaichiko,
Saeki-ku, Hiroshima 731-5161, Japan

A Nonsmooth Quasi-Static Modeling Approach for Hydraulic Actuators

This paper presents an analytical approach for modeling the quasi-static characteristics of hydraulic actuators driven by four-valve independent metering circuits. The presented model is described as a nonsmooth, set-valued function from the velocity to the set of forces with which the equilibrium is achieved at the velocity. It is derived from algebraic relations among the velocity of the actuator, the steady-state force generated by the actuator, and the flowrate and the steady-state pressure at all valves in the circuit. This approach is also applied to more involving circuits including a regeneration pipeline and those with multiple actuators. The contribution of the paper can be seen as an example case study of the fact that these complicated circuit structures are analytically tractable through an extension of the conventional hydraulic–electric analogy. The obtained analytical expressions of the steady-state velocity–force relations allow for concise visualization of the actuators' characteristics. [DOI: 10.1115/1.4051894]

1 Introduction

Construction machines require continuing research on the control technology for future applications, such as remote and semi-automatic operations. Physical models of the construction machines are necessary for developing sophisticated controllers, observers, and simulators. In particular, hydraulic actuators and hydraulic circuits are important components of construction machines, of which the physical behaviors need to be appropriately modeled. The behavior of a hydraulic actuator is highly involving, depending on the oil supply from the pump, the external forces acting on the actuator, and the states and the characteristics of many valves in the circuit.

A straightforward approach for modeling a hydraulic actuator is to construct a quasi-static[1] map from the steady-state velocity to the actuator force. The force–velocity maps can be derived from the balance between the flowrate and pressure at the valves, depending on the valve openings. Such an approach is quite classical and is often referred to as the hydraulic–electric analogy [1–4], which replaces the pressure and the flowrate by the voltage and the current, respectively. Some researchers constructed controllers in this approach [5–12], but its application is limited to relatively simple circuits that do not involve many valves.

A more physically accurate modeling approach is to consider the first-order dynamics of the pressure. In such an approach, the circuit is often divided into several oil volumes, such as those in the circuit pipelines and the actuator chambers. In each volume, the pressure is determined by a first-order differential equation depending on the oil flowrates in and out of the volume. It is sometimes referred to as a lumped fluid approach and has been employed for the controller design [13–16] and for simulation purposes [17,18]. Although this approach can be applied to complicated circuits with many valves, because of the high bulk modulus of the oil, the differential equations can be numerically stiff, and thus it usually demands a small time-step and high computational cost. In addition, it requires iterative computation to obtain the steady-state force–velocity relations.

This paper presents an approach for deriving mathematical representations of quasi-static force–velocity relations of hydraulic actuators with relatively complicated circuits. The circuit structure shown in Fig. 1 is used as an example, being motivated by those used in commercial hydraulic excavators. This approach focuses on the quasi-static balance between the flowrate and the pressure, which is the equilibrium of the first-order pressure dynamics. More specifically, at the steady-state, the pressure difference across each valve determines the oil flowrate through the valve, the oil flowrate into the actuator determines the actuator's velocity, the pressures in the actuator chambers determine the force generated by the actuator, and the generated force equals the external force acting on the actuator. This paper elaborates an analytical expression of the steady-state relation between the actuator velocity and the external force from the quasi-static

[1]We use the term "quasi-static" because the model does not involve the pressure dynamics but involves the motion of the actuator and the oil.

Contributed by the Dynamic Systems Division of ASME for publication in the Journal of Dynamic Systems, Measurement, and Control. Manuscript received March 12, 2021; final manuscript received July 13, 2021; published online September 13, 2021. Assoc. Editor: Tatiana Minav.

representations of all valves in the circuit. One important feature of the presented expression is that it is nonsmooth, allowing for the set-valuedness[2] of the force–velocity map especially when the valves are closed or the actuator is stopped.

The presented nonsmooth formalism can be seen as one form of the classical hydraulic–electric analogy [1–4], and it is also analogous to the *nonsmooth electronics* [19–21]. From another perspective, the presented approach is close to those of some previous papers [22–24] that apply the singular perturbation theory to the dynamical models of hydraulic systems. In their approach, the terms including the pressure rate-of-changes are removed from the dynamical models assuming that the pressure dynamics is sufficiently fast. In contrast to their approaches, the presented nonsmooth approach allows for multiple steady-states by involving the set-valuedness.

In general, many force-exerting devices can be characterized by quasi-static maps from the velocity to the force [25,26], which can be used by engineers to choose devices that meet their requirements. The presented approach provides such quasi-static maps of hydraulic actuators as closed-form analytical expressions, which do not require iterative computation. The obtained quasi-static map would also be useful as a nominal plant model to be used in the design of controllers and observers, as has been the case with relatively simpler circuits [5–12]. In addition, the map would be used as a basis to construct a new dynamical model for simulation purposes by including additional terms involving time derivatives.

This paper is organized as follows. Section 2 shows mathematical preliminaries, including definitions of relevant functions and some theorems. Section 3 constructs a nonsmooth representation of the quasi-static characteristics of the hydraulic circuit of Fig. 1, which describes the algebraic relation among the valve openings, the rod velocity, and the external force. Section 4 presents an extension of the approach to include a regeneration pipeline, and Sec. 5 presents another extension to include multiple actuators driven by a single pump. Section 6 provides some concluding remarks.

2 Mathematical Preliminary

In this paper, $\mathbb{R}$ denotes the set of all real numbers. This paper extensively uses mathematical notations of the nonsmooth system theory, which involves set-valued functions. We use the following set-valued functions:

$$\mathcal{N}_{[A,B]}(x) \triangleq \begin{cases} [0,\infty) & \text{if } x = B \\ 0 & \text{if } x \in (A,B) \\ (-\infty,0] & \text{if } x = A \\ \varnothing & \text{otherwise} \end{cases} \tag{1}$$

$$\mathrm{gsgn}(a,x,b) \triangleq \begin{cases} b & \text{if } x > 0 \\ \mathrm{conv}\{a,b\} & \text{if } x = 0 \\ a & \text{if } x < 0 \end{cases} \tag{2}$$

The definition (1) assumes $A < B$. Here, $\mathrm{conv}\{a,b\}$ stands for the convex closure of the set $\{a, b\}$, being the closed set $[a,b]$ if $a \le b$ and $[b,a]$ if $b \le a$. The function $\mathcal{N}_{\mathcal{A}}(x)$ is referred to as the normal cone of the set $\mathcal{A}$ at the point x. The function gsgn can be seen as a generalized version of the set-valued signum function. With the normal cone $\mathcal{N}$, the following relation holds true:

$$\begin{aligned} 0 \le x \perp y \ge 0 \quad &\Longleftrightarrow \quad x \in -\mathcal{N}_{[0,\infty)}(y) \\ &\Longleftrightarrow \quad y \in -\mathcal{N}_{[0,\infty)}(x) \end{aligned} \tag{3}$$

Each of the above three expressions means that x and y are nonpositive scalars at least one of which is zero. This relation is convenient to describe the flowrate–pressure relation at check valves. In addition, with $A < B$, the following relation holds true:

$$y \in \mathcal{N}_{[A,B]}(x) \iff x \in \mathrm{gsgn}(A,y,B) \tag{4}$$

The following function represents the projection onto a closed set:

$$\mathrm{proj}_{[A,B]}(\mathrm{x}) \triangleq \max(A, \min(B,x)) \tag{5}$$

where $A < B$. The normal cone and the projection have the following relation:

$$a - x \in \mathcal{N}_{\mathcal{A}}(x) \iff x = \mathrm{proj}_{\mathcal{A}}(a) \tag{6}$$

which has been shown in previous publications (e.g., Refs. [27, Proposition 2], [28, Section A.3], and [29, Proposition 6.47]). This paper uses the following theorem:

THEOREM 1. *Let $x \in \mathbb{R}$ and let $\mathcal{A} \subset \mathbb{R}$ be a closed convex subset of $\mathbb{R}$. Let $f : \mathbb{R} \to \mathbb{R}$ be a strictly decreasing continuous function. Let $x_f \in \mathbb{R}$ satisfy $f(x_f) = 0$. Then, the following statement holds true:*

$$f(x) \in \mathcal{N}_{\mathcal{A}}(x) \iff x = \mathrm{proj}_{\mathcal{A}}(x_f) \tag{7}$$

Proof. Because f is strictly decreasing, $x < x_f \Longleftrightarrow f(x) > 0$, $x > x_f \Longleftrightarrow f(x) < 0$, and $x = x_f \Longleftrightarrow f(x) = 0$ are satisfied. This means that $f(x) \in \mathcal{N}_{\mathcal{A}}(x) \Longleftrightarrow x_f - x \in \mathcal{N}_{\mathcal{A}}(x)$ and Eq. (6) implies that it is equivalent to $x = \mathrm{proj}_{\mathcal{A}}(x_f)$. ■

The following single-valued functions are used in the paper:

$$\mathcal{S}(x) \triangleq \mathrm{sgn}(x)x^2 \tag{8}$$

$$\mathcal{R}(x) \triangleq \mathrm{sgn}(\mathrm{x})\sqrt{|x|} \tag{9}$$

The functions $\mathcal{R}$ and $\mathcal{S}$ are strictly increasing continuous functions satisfying $\mathcal{R}(\mathcal{S}(x)) = \mathcal{S}(\mathcal{R}(x)) = x$.

3 Nonsmooth Quasi-Static Model

3.1 Problem Setting. This section considers the hydraulic circuit illustrated in Fig. 1, which is a four-valve independent metering circuit to drive a double-acting hydraulic actuator, being motivated by the circuits used in commercial hydraulic

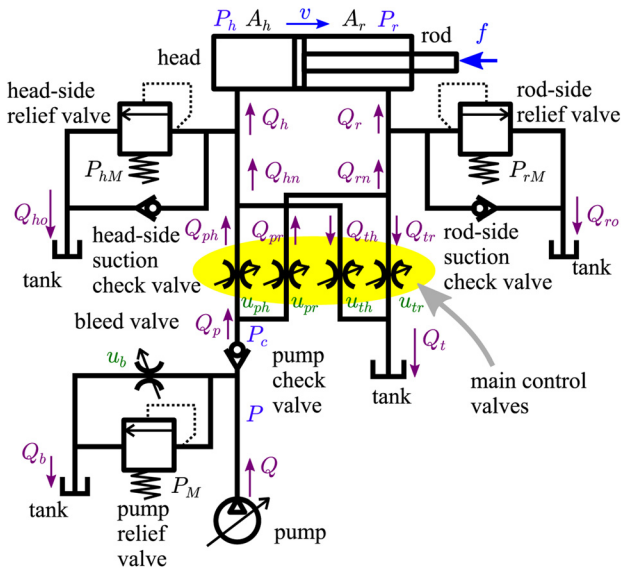

Fig. 1 Hydraulic actuator and its circuit

[2]A function is said to be set-valued, as opposed to single-valued, if its return value can be a set of values, as opposed to a single value. A set-valued function is also said to be nonsmooth if it is not differentiable at some points.

excavators. The actuator has two chambers separated by the piston, and the motion of the piston is extracted as the motion of the rod, which applies forces to external objects. We are interested in the quasi-static relation among the rod velocity v, positive when the rod is extending, the external force f, positive when it is compressing the rod, and the opening ratios of the valves.

The hydraulic circuit in Fig. 1 is similar to those studied in, e.g., Refs. [5–12] and [30], where the quasi-static relations are also considered. They however focus on rather simplified cases where relief valves and check valves are neglected. Our main contribution lies in an elaborate analytical representation of the whole circuit, which is rather complicated than those in previous studies, using the nonsmooth formalism to deal with relief valves and check valves.

Although the circuit of Fig. 1 looks complicated, its configuration can be seen as almost minimal from a practical point of view. For example, the relief valves and the suction check valves connected to the chambers are essential to prevent excessively high pressure in the chambers. The pump relief valve and the bleed valve are also essential to secure the oil outlet from the pump when the main control valves are closed. The pump check valve is necessary to prevent the backflow into the pump, which may happen when the velocity opposes the exerted force of the actuator. Previous papers exclude these components by imposing assumptions on the combination of the speed and the valve openings. In contrast, this paper aims to derive a single, unified representation that holds with any combinations of the velocity and valve openings.

This paper uses the terminology for linear hydraulic actuators (i.e., hydraulic cylinders), but the presented approach is also applicable to rotary hydraulic actuators by replacing the velocity and the external force by the angular velocity and the torque, respectively.

3.2 Quasi-Static Relations. In Fig. 1, Q_* and P_* denote the flowrates and the pressure at each point. The pump provides the flowrate Q to the circuit via a pump check valve and two of the four main control valves. These control valves are connected to the head-side and the rod-side chambers of the actuator. The chambers are also connected to the tank with the zero pressure via the other two control valves. Each chamber of the actuator also connects to the tank through a parallel combination of a relief valve and a check valve, which are named as indicated in the figure. There is another control valve, referred to as a bleed valve, and it leads to the tank in parallel to a relief valve, referred to as a pump relief valve.

The degrees of the opening of the valves are represented by dimensionless variables $u_* \in [0,1]$ $(* \in \{ph, tr, pr, th, b\})$, which are the ratios of the valve opening areas to their maximum values. The control valves are manipulated by a controller that accepts external commands, which are given through, e.g., operation levers of an excavator. When the external command is to stop the actuator, all the four main valves are closed. When the external command is to move the actuator in the positive direction (i.e., extend the rod), both or either of u_{ph} and u_{tr} are set positive and u_{th} and u_{pr} are set zero. When the operator's command is to move the actuator in the negative direction (i.e., retract the rod), u_{ph} and u_{tr} are set zero and both or either of u_{th} and u_{pr} are set positive. Based on this idea, we assume that the vector $\boldsymbol{u} \triangleq [u_{ph}, u_{tr}, u_{pr}, u_{th}, u_b]^T$ always belongs to either of the following three subsets:

$$\mathcal{U}_0 \triangleq \{\boldsymbol{u} \in \mathbb{R}^5 \mid u_1 = u_2 = u_3 = u_4 = 0 \wedge u_5 > 0\} \tag{10a}$$

$$\mathcal{U}_+ \triangleq \{\boldsymbol{u} \in \mathbb{R}^5 \mid u_1^2 + u_2^2 > 0 \wedge u_3 = u_4 = 0 \wedge u_5 \geq 0\} \tag{10b}$$

$$\mathcal{U}_- \triangleq \{\boldsymbol{u} \in \mathbb{R}^5 \mid u_1 = u_2 = 0 \wedge u_3^2 + u_4^2 > 0 \wedge u_5 \geq 0\} \tag{10c}$$

where u_i $(i \in \{1, \ldots, 5\})$ stands for the ith element of the vector $\boldsymbol{u}$.

Now, let us make an exhaustive list of algebraic relations among the pressures, the flowrates, the external force, and the actuator velocity at the steady-state. First, according to the principle of mass conservation, which is analogous to Kirchhoff's law in electric circuits, one can see that the following relations hold true at junctions in the circuit:

$$Q_{hn} = Q_{ph} - Q_{th} \tag{11a}$$

$$Q_{rn} = Q_{pr} - Q_{tr} \tag{11b}$$

$$Q_h = Q_{hn} - Q_{ho} \tag{11c}$$

$$Q_r = Q_{rn} - Q_{ro} \tag{11d}$$

$$Q_t = Q_{th} + Q_{tr} \tag{11e}$$

$$Q_p = Q_{ph} + Q_{pr} \tag{11f}$$

$$Q_b = Q - Q_p \tag{11g}$$

Second, let us focus on the control valves. As indicated in Fig. 1, P_h and P_r are the internal pressures of the head- and rod-side chambers, respectively, P_c is the pressure at the check valve connected to the pump, and P is the pressure at the outlet of the pump. According to the conventional orifice model [14,31], we can assume that the following flowrate–pressure relations are satisfied:

$$Q_{ph} = c_{ph} u_{ph} \mathcal{R}(P_c - P_h) \tag{11h}$$

$$Q_{th} = c_{th} u_{th} \mathcal{R}(P_h) \tag{11i}$$

$$Q_{pr} = c_{pr} u_{pr} \mathcal{R}(P_c - P_r) \tag{11j}$$

$$Q_{tr} = c_{tr} u_{tr} \mathcal{R}(P_r) \tag{11k}$$

$$Q_b \in c_b u_b \mathcal{R}(P) + \mathcal{N}_{(-\infty, P_M]}(P) \tag{11l}$$

Figure 2(*a*) illustrates the relation (11*h*). The coefficients c_* are defined as $c_* = C_* a_* \sqrt{2/\rho}$ $(* \in \{ph, tr, pr, th, b\})$, where C_* is the dimensionless coefficient named a discharge coefficient [32], which is typically around 0.6 or 0.7 [33,34], a_* is the maximum opening area (m^2) of the valve, and ρ is the mass density (kg/m^3) of the oil. Equation (11*l*) represents the combined effect of the relief valve and the bleed valve, which limits the pump pressure up to P_M as illustrated in Fig. 2(*b*).

Third, let us consider the check valves and the relief valves. The check valve connected to the pump imposes the following constraint:

$$Q_p \in -\mathcal{N}_{[0,\infty)}(P_c - P) \tag{11m}$$

which means that the flowrate Q_p is zero when $P_c - P > 0$, as illustrated in Fig. 2(*c*). It can be seen as analogous to the ideal diode [19] in electric circuits. The effects of the relief valves and the suction check valves connected to the chambers are written as follows:

$$Q_{ho} \in \mathcal{N}_{[0,P_{hM}]}(P_h) \tag{11n}$$

$$Q_{ro} \in \mathcal{N}_{[0,P_{rM}]}(P_r) \tag{11o}$$

Here, P_{hM} and P_{rM} are the pressure limits of the relief valves connected to the head- and rod-side chambers, respectively. These expressions mean that P_h and P_r are always in the ranges of $[0, P_{hM}]$ and $[0, P_{rM}]$, respectively, as illustrated in Fig. 2(*d*). When the pressure reaches the upper limit, the oil flows into the

tank. When the pressure reaches zero, the oil is drawn into the chamber from the tank.

Finally, we discuss the actuator. Let A_h and A_r be the cross-sectional areas of the head- and rod-side chambers, respectively. Then, at the steady-state where the rod inertia can be neglected, the constraints imposed by the actuator can be written as follows:

$$v = Q_h/A_h \tag{11p}$$

$$v = -Q_r/A_r \tag{11q}$$

$$f = A_h P_h - A_r P_r \tag{11r}$$

If one deals with rotary actuators, both A_r and A_h (measured in m^2) should be replaced by the volume displacement per one radian of rotation, which is measured in m^3/rad.

In conclusion, now we have 18 algebraic constraints in Eq. (11) and 19 variables, which are 13 flowrate values (Q_{ho}, Q_{ro}, Q_{hn}, Q_{rn}, Q_h, Q_r, Q_{ph}, Q_{pr}, Q_{th}, Q_{tr}, Q_t, Q_p, and Q_b), four pressure values (P, P_h, P_r, and P_c), the external force (f) to the rod, and the velocity (v) of the rod.

For the convenience of derivation, we now normalize some quantities in the following manner:

$$q_* \triangleq Q_*/A_h (* \in \{ho, hn, h, ph, th\}) \tag{12}$$

$$\widehat{u}_* \triangleq c_* u_*/A_h^{3/2} (* \in \{ph, th\}) \tag{13}$$

$$q_* \triangleq Q_*/A_r (* \in \{ro, rn, r, pr, tr\}) \tag{14}$$

$$\widehat{u}_* \triangleq c_* u_*/A_r^{3/2} (* \in \{pr, tr\}) \tag{15}$$

$$F_* \triangleq P_* A_*, \quad F_{*M} \triangleq P_{*M} A_* (* \in \{h, r\}) \tag{16}$$

$$U_b \triangleq c_b u_b \tag{17}$$

The regularized input vector is defined as $\widehat{\boldsymbol{u}} = [\widehat{u}_{ph}, \widehat{u}_{tr}, \widehat{u}_{pr}, \widehat{u}_{th}, U_b]^T$. By using these definitions, Eq. (11) can be rewritten as follows:

$$q_{hn} = q_{ph} - q_{th} \tag{18a}$$

$$q_{rn} = q_{pr} - q_{tr} \tag{18b}$$

$$q_h = q_{hn} - q_{ho} \tag{18c}$$

$$q_r = q_{rn} - q_{ro} \tag{18d}$$

$$Q_t = A_h q_{th} + A_r q_{tr} \tag{18e}$$

$$Q_p = A_h q_{ph} + A_r q_{pr} \tag{18f}$$

$$Q_b = Q - Q_p \tag{18g}$$

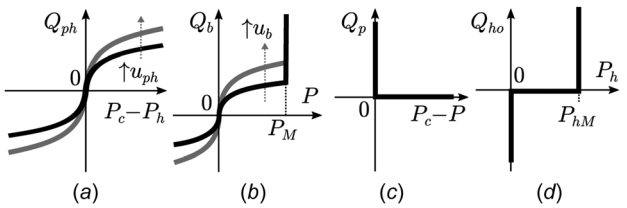

Fig. 2 Flowrate–pressure relations at (*a*) one of main control valves (11*h*), (*b*) the bleed and the pump relief valves (11*l*), (*c*) the pump check valve (11*m*), and (*d*) the head-side relief and the suction check valves (11*n*)

$$q_{ph} = \widehat{u}_{ph} \mathcal{R}(A_h P_c - F_h) \tag{18h}$$

$$q_{th} = \widehat{u}_{th} \mathcal{R}(F_h) \tag{18i}$$

$$q_{pr} = \widehat{u}_{pr} \mathcal{R}(A_r P_c - F_r) \tag{18j}$$

$$q_{tr} = \widehat{u}_{tr} \mathcal{R}(F_r) \tag{18k}$$

$$Q_b \in U_b \mathcal{R}(P) + \mathcal{N}_{(-\infty, P_M]}(P) \tag{18l}$$

$$Q_p \in \mathcal{N}_{(-\infty, P_c]}(P) \tag{18m}$$

$$q_{ho} \in \mathcal{N}_{[0, F_{hM}]}(F_h) \tag{18n}$$

$$q_{ro} \in \mathcal{N}_{[0, F_{rM}]}(F_r) \tag{18o}$$

$$v = q_h \tag{18p}$$

$$v = -q_r \tag{18q}$$

$$f = F_h - F_r \tag{18r}$$

Note that the equivalence between Eqs. (11*m*) and (18*m*) can be derived from the definition of the normal cone.

3.3 Some Derivations to Obtain F_h and F_r. Now, let us attempt to reduce the number of variables. Substituting Eqs. (18*m*) and (18*g*) into Eq. (18*l*) yields

$$\begin{aligned} Q \in \mathcal{N}_{(-\infty, P_c]}(P) + U_b \mathcal{R}(P) + \mathcal{N}_{(-\infty, P_M]}(P) \\ = U_b \mathcal{R}(P) + \mathcal{N}_{(-\infty, \min(P_c, P_M)]}(P) \end{aligned} \tag{19}$$

which is equivalent to

$$P = \min(P_c, P_M, \mathcal{S}(Q/U_b)) \tag{20}$$

because of Theorem 1. Since $q_h = -q_r = v$, we can eliminate the two variables q_h and q_r. Moreover, q_{ho}, q_{ro}, q_{hn}, q_{rn}, q_{ph}, q_{th}, q_{pr}, q_{tr}, and Q_t can also be eliminated. This gives the following five equations for the five variables $\{P, P_c, F_h, F_r, f\}$:

$$-v + \widehat{u}_{ph} \mathcal{R}(A_h P_c - F_h) - \widehat{u}_{th} \mathcal{R}(F_h) \in \mathcal{N}_{[0, F_{hM}]}(F_h) \tag{21a}$$

$$v + \widehat{u}_{pr} \mathcal{R}(A_r P_c - F_r) - \widehat{u}_{tr} \mathcal{R}(F_r) \in \mathcal{N}_{[0, F_{rM}]}(F_r) \tag{21b}$$

$$A_h \widehat{u}_{ph} \mathcal{R}(A_h P_c - F_h) + A_r \widehat{u}_{pr} \mathcal{R}(A_r P_c - F_r) \in \mathcal{N}_{(-\infty, P_c]}(P) \tag{21c}$$

$$\begin{aligned} Q \in U_b \mathcal{R}(P) + A_h \widehat{u}_{ph} \mathcal{R}(A_h P_c - F_h) \\ + A_r \widehat{u}_{pr} \mathcal{R}(A_r P_c - F_r) + \mathcal{N}_{(-\infty, P_M]}(P) \end{aligned} \tag{21d}$$

and

$$f = F_h - F_r \tag{22}$$

Now we derive the relation between v and $\{F_h, F_r\}$ from Eq. (21). If $\widehat{\boldsymbol{u}} \in \mathcal{U}_0$, Eq. (21) reduces to the following:

$$-v \in \mathcal{N}_{[0, F_{hM}]}(F_h) \tag{23a}$$

$$v \in \mathcal{N}_{[0, F_{rM}]}(F_r) \tag{23b}$$

$$0 \in \mathcal{N}_{(-\infty, P_c]}(P) \tag{23c}$$

$$Q \in U_b \mathcal{R}(P) + \mathcal{N}_{(-\infty, P_M]}(P) \tag{23d}$$

from which

$$F_h \in \mathrm{gsgn}(F_{hM}, v, 0), \quad F_r \in \mathrm{gsgn}(0, v, F_{rM}) \tag{24}$$

can be derived by using Eq. (4). This means that f can take any values between F_{hM} and $-F_{rM}$ when $v=0$, which is consistent with the fact that, when all the main control valves are closed, the cylinder holds its position by producing the reaction force against the external force as long as the relief valves are closed.

When $\widehat{\boldsymbol{u}} \in \mathcal{U}_+$, Eq. (21) reduces to the following:

$$-v + \widehat{u}_{ph}\mathcal{R}(A_hP_c - F_h) \in \mathcal{N}_{[0,F_{hM}]}(F_h) \tag{25a}$$

$$v - \widehat{u}_{tr}\mathcal{R}(F_r) \in \mathcal{N}_{[0,F_{rM}]}(F_r) \tag{25b}$$

$$A_h\widehat{u}_{ph}\mathcal{R}(A_hP_c - F_h) \in \mathcal{N}_{(-\infty,P_c]}(P) \tag{25c}$$

$$Q \in U_b\mathcal{R}(P) + A_h\widehat{u}_{ph}\mathcal{R}(A_hP_c - F_h) + \mathcal{N}_{(-\infty,P_M]}(P) \tag{25d}$$

By careful derivation detailed in the Appendix, one can eliminate P and P_c from Eq. (25) to obtain the following:

$$F_h \in \mathrm{gsgn}\Big(F_{hM}, v, \mathrm{proj}_{[0,F_{hM}]}\big(\min\big(A_hP_M, -\frac{A_h^3}{U_b^2}\mathcal{S}\Big(v - \frac{Q}{A_h}\Big)\big) - \frac{\mathcal{S}(v)}{\widehat{u}_{ph}^2}\big)\Big) \tag{26a}$$

$$F_r = \mathrm{proj}_{[0,F_{rM}]}\Big(\mathcal{S}(v)/\widehat{u}_{tr}^2\Big) \tag{26b}$$

When $\widehat{\boldsymbol{u}} \in \mathcal{U}_-$, in the same manner, we have the following:

$$F_h = \mathrm{proj}_{[0,F_{hM}]}\Big(-\mathcal{S}(v)/\widehat{u}_{th}^2\Big) \tag{27a}$$

$$F_r \in \mathrm{gsgn}\left(\mathrm{proj}_{[0,F_{rM}]}\left(\min\left(A_rP_M, \frac{A_r^3}{U_b^2}\mathcal{S}\Big(v + \frac{Q}{A_r}\Big)\right) + \frac{\mathcal{S}(v)}{\widehat{u}_{pr}^2}\right), v, F_{rM}\right) \tag{27b}$$

3.4 Main Result: Nonsmooth Quasi-Static Map From v to f. Now we are in position to derive the relation between the force f and the velocity v. Combining Eq. (24) for $\widehat{\boldsymbol{u}} \in \mathcal{U}_0$, Eq. (26) for $\widehat{\boldsymbol{u}} \in \mathcal{U}_+$, and Eq. (27) for $\widehat{\boldsymbol{u}} \in \mathcal{U}_-$ results in the following:

$$F_h \in \Gamma_h(v) \triangleq \mathrm{gsgn}(\Gamma_{h-}(v), v, \Gamma_{h+}(v)) \tag{28a}$$

$$F_r \in \Gamma_r(v) \triangleq \mathrm{gsgn}(\Gamma_{r-}(v), v, \Gamma_{r+}(v)) \tag{28b}$$

where

$$\Gamma_{h+}(v) \triangleq \mathrm{proj}_{[0,F_{hM}]}\left(\min\left(A_hP_M, -\frac{A_h^3}{U_b^2}\mathcal{S}\Big(v - \frac{Q}{A_h}\Big)\right) - \frac{\mathcal{S}(v)}{\widehat{u}_{ph}^2}\right) \tag{28c}$$

$$\Gamma_{h-}(v) \triangleq \mathrm{proj}_{[0,F_{hM}]}\quad -\frac{\mathcal{S}(v)}{\widehat{u}_{th}^2}\Big) \tag{28d}$$

$$\Gamma_{r+}(v) \triangleq \mathrm{proj}_{[0,F_{rM}]}\left(\frac{\mathcal{S}(v)}{\widehat{u}_{tr}^2}\right) \tag{28e}$$

$$\Gamma_{r-}(v) \triangleq \mathrm{proj}_{[0,F_{rM}]}\left(\min\left(A_rP_M, \frac{A_r^3}{U_b^2}\mathcal{S}\Big(v + \frac{Q}{A_r}\Big)\right) + \frac{\mathcal{S}(v)}{\widehat{u}_{pr}^2}\right) \tag{28f}$$

By using Eqs. (22) and (28), the relation between v and f is obtained as follows:

$$f \in \Gamma(v) \triangleq \Gamma_h(v) - \Gamma_r(v) \tag{29}$$

For the convenience of further derivations, we can also write the set-valued map $\Gamma(v)$ in the following form:

$$\Gamma(v) = \mathrm{gsgn}(\Gamma_-(v), v, \Gamma_+(v)) \tag{30a}$$

where

$$\begin{aligned}\Gamma_+(v) &\triangleq \Gamma_{h+}(v) - \Gamma_{r+}(v)\\ &= \max(\min(\max(\Gamma_{+0a}(v), \Gamma_{+0b}(v)),\\ &\quad \max(\Gamma_{+1a}(v), \Gamma_{+1b}(v)),\\ &\quad \max(\Gamma_{+2a}(v), \Gamma_{+2b}(v))), \quad \Gamma_{+3}(v), -F_{rM})\end{aligned} \tag{30b}$$

$$\begin{aligned}\Gamma_-(v) &\triangleq \Gamma_{h-}(v) - \Gamma_{r-}(v)\\ &= \min(\max(\min(\Gamma_{-0a}(v), \Gamma_{-0b}(v)),\end{aligned} \tag{30c}$$

$$\begin{aligned}\Gamma_-(v) &\triangleq \Gamma_{h-}(v) - \Gamma_{r-}(v)\\ &= \min(\max(\min(\Gamma_{-0a}(v), \Gamma_{-0b}(v)),\\ &\quad \min(\Gamma_{-1a}(v), \Gamma_{-1b}(v)),\\ &\quad \min(\Gamma_{-2a}(v), \Gamma_{-2b}(v))), \Gamma_{-3}(v), F_{hM})\end{aligned} \tag{30c}$$

$$\Gamma_{+0a}(v) \triangleq F_{hM} - \frac{\mathcal{S}(v)}{\widehat{u}_{tr}^2} \tag{30d}$$

$$\Gamma_{+0b}(v) \triangleq F_{hM} - F_{rM} \tag{30e}$$

$$\Gamma_{+1a}(v) \triangleq -\frac{A_h^3}{U_b^2}\mathcal{S}\Big(v - \frac{Q}{A_h}\Big) - \frac{\mathcal{S}(v)}{\widehat{u}_{ph}^2} - \frac{\mathcal{S}(v)}{\widehat{u}_{tr}^2} \tag{30f}$$

$$\Gamma_{+1b}(v) \triangleq -\frac{A_h^3}{U_b^2}\mathcal{S}\Big(v - \frac{Q}{A_h}\Big) - \frac{\mathcal{S}(v)}{\widehat{u}_{ph}^2} - F_{rM} \tag{30g}$$

$$\Gamma_{+2a}(v) \triangleq A_hP_M - \frac{\mathcal{S}(v)}{\widehat{u}_{ph}^2} - \frac{\mathcal{S}(v)}{\widehat{u}_{tr}^2} \tag{30h}$$

$$\Gamma_{+2b}(v) \triangleq A_hP_M - \frac{\mathcal{S}(v)}{\widehat{u}_{ph}^2} - F_{rM} \tag{30i}$$

$$\Gamma_{+3}(v) \triangleq -\frac{\mathcal{S}(v)}{\widehat{u}_{tr}^2} \tag{30j}$$

$$\Gamma_{-0a}(v) \triangleq -F_{rM} - \frac{\mathcal{S}(v)}{\widehat{u}_{th}^2} \tag{30k}$$

$$\Gamma_{-0b}(v) \triangleq -F_{rM} + F_{hM} \tag{30l}$$

$$\Gamma_{-1a}(v) \triangleq -\frac{A_r^3}{U_b^2}\mathcal{S}\Big(v + \frac{Q}{A_r}\Big) - \frac{\mathcal{S}(v)}{\widehat{u}_{pr}^2} - \frac{\mathcal{S}(v)}{\widehat{u}_{th}^2} \tag{30m}$$

$$\Gamma_{-1b}(v) \triangleq -\frac{A_r^3}{U_b^2}\mathcal{S}\Big(v + \frac{Q}{A_r}\Big) - \frac{\mathcal{S}(v)}{\widehat{u}_{pr}^2} + F_{hM} \tag{30n}$$

$$\Gamma_{-2a}(v) \triangleq -A_rP_M - \frac{\mathcal{S}(v)}{\widehat{u}_{pr}^2} - \frac{\mathcal{S}(v)}{\widehat{u}_{th}^2} \tag{30o}$$

$$\Gamma_{-2b}(v) \triangleq -A_r P_M - \frac{\mathcal{S}(v)}{\widehat{u}_{pr}^2} + F_{hM} \tag{30p}$$

$$\Gamma_{-3}(v) \triangleq -\frac{\mathcal{S}(v)}{\widehat{u}_{th}^2} \tag{30q}$$

Here, the divisions by $\widehat{u}_*^2$ or U_b^2 do not cause troubles even when they are zeros because Eq. (30*b*) implicitly includes upper and lower bounds. One workaround in the use in computer programs may be to replace the divisions by $\widehat{u}_*^2$ by those by $\max\left(\varepsilon, \widehat{u}_*^2\right)$ where ε is a small positive number close to the machine epsilon.

It should be noted that, at $v = 0$, the function $\Gamma(v)$ is set-valued and its value is the closed set $[\Gamma_+(0), \Gamma_-(0)]$. The boundaries $\Gamma_+(0)$ and $\Gamma_-(0)$ are obtained from a straightforward derivation as

$$\begin{aligned} \Gamma_+(0) &= \Gamma_{h+}(0) - \Gamma_{r+}(0) \\ \Gamma_-(0) &= \Gamma_{h-}(0) - \Gamma_{r-}(0) \end{aligned} \tag{31a}$$

where

$$\Gamma_{h+}(0) = \begin{cases} \min\left(F_{hM}, A_h P_M, A_h Q^2 / U_b^2\right) & \text{if } \widehat{u}_{ph} > 0 \\ 0 & \text{if } \widehat{u}_{ph} = 0 \end{cases} \tag{31b}$$

$$\Gamma_{r+}(0) = \begin{cases} 0 & \text{if } \widehat{u}_{tr} > 0 \\ F_{rM} & \text{if } \widehat{u}_{tr} = 0 \end{cases} \tag{31c}$$

$$\Gamma_{h-}(0) = \begin{cases} 0 & \text{if } \widehat{u}_{th} > 0 \\ F_{hM} & \text{if } \widehat{u}_{th} = 0 \end{cases} \tag{31d}$$

$$\Gamma_{r-}(0) = \begin{cases} \min\left(F_{rM}, A_r P_M, A_r Q^2 / U_b^2\right) & \text{if } \widehat{u}_{pr} > 0 \\ 0 & \text{if } \widehat{u}_{pr} = 0 \end{cases} \tag{31e}$$

As can be seen from the expression (30), the function $\Gamma(v)$ is composed of many segments. Interestingly, each segment has a clear physical interpretation. For example, in the segments listed in Eqs. (30*d*)–(30*j*), the last term, either $-F_{rM}$ or $-\mathcal{S}(v)/\widehat{u}_{tr}^2$, represents the state of the rod-side relief valve, either closed or open, respectively. In this way of consideration, we can summarize the valve states at each curve segment as in Table 1. Such direct correspondence between the mathematical representation and the valve states would help analytically understanding the physical characteristics of the actuator.

3.5 Numerical Examples. Some numerical examples are now presented. We consider an asymmetric hydraulic cylinder with the following parameter values:

$$\begin{aligned} &C_* = 0.6,\ a_* = 0.0001\,\mathrm{m}^2,\ \rho = 850\,\mathrm{kg/m}^3 \\ &\mathrm{A_h} = 0.024\,\mathrm{m}^2, A_r = 0.012\,\mathrm{m}^2 \\ &P_{hM} = 42\,\mathrm{MPa},\ P_{rM} = 40\,\mathrm{MPa},\ P_M = 36\,\mathrm{MPa} \\ &Q = 500\,\mathrm{L/min} = 0.00833\,\mathrm{m}^3/\mathrm{s} \end{aligned} \tag{32}$$

A common control command $u_c \in [-1, 1]$ is used to set the openings of the main control valves as follows:

$$\begin{aligned} u_{ph} = u_{tr} &= \max(u_c, 0) \\ u_{pr} = u_{th} &= \max(-u_c, 0) \end{aligned} \tag{33}$$

The opening of the bleed valve was fixed at $u_b = 0.2$ unless otherwise noted.

Results with different values of u_c and u_b are shown in Fig. 3. Figure 3(*a*) shows the function Γ and its segments with a positive u_c, while Fig. 3(*b*) shows those with a negative u_c. They show that $\Gamma(v)$ is always a decreasing function of v and it is set-valued at $v = 0$. Figure 3(*c*) shows how the function $\Gamma(v)$ varies according to the change in u_c. It shows that, at a constant external force, the velocity v increases as u_c increases, which is consistent with the behavior of real hydraulic actuators. Figure 3(*d*) shows that the velocity v decreases as the bleed valve opening u_b increases. It can be explained by the fact that the oil flow into the actuator decreases as the bleed valve opens. In addition, Fig. 4 is a three-dimensional plot of $f \in \Gamma(v)$ with different u_c values, which is another representation of the data in Fig. 3(*c*). The set-valuedness of Γ is visible as a vertical line or vertical walls in Fig. 4.

It should be emphasized that dynamical models considering the pressure dynamics of small oil volumes in the circuits would demand iterative computation to obtain the steady-state characteristics such as those illustrated in Figs. 3 and 4, while they are obtained analytically from the presented quasi-static model. Conversely, the presented quasi-static representation may be extended into a dynamical model, e.g., by including the first-order pressure dynamics with appropriate time constants, considering that dynamics models of various systems are often obtained as extensions of static or steady-state models.

4 Extension 1: Regeneration Circuit

In some practical applications, the circuit of Fig. 1 includes an additional pathway from the rod-side chamber to the head-side chamber to make the extending movement faster. This section considers the circuit of Fig. 5, which is an extension of the circuit of Fig. 1. We assume that the regeneration pipeline has a valve that flows only from the head side to the rod side and assume that the cross-sectional areas of the cylinder satisfy

$$A_h \geq A_r \tag{34}$$

There must be some cylinders that do not satisfy Eq. (34), but this paper focuses on this case for brevity. Let a_a is the maximum opening area (m^2) of the regeneration valve, and let $u_a \in [0, 1]$ be the dimensionless input value, which is the ratio of the valve opening area to its maximum value a_a. Then, the flowrate of the oil through the regeneration pipeline is written as follows:

$$Q_a = c_a u_a \max(\mathcal{R}(F_r/A_r - F_h/A_h, 0)) \tag{35}$$

where $c_a \triangleq C_a a_a \sqrt{2/\rho}$ and C_a is the discharge coefficient of the regeneration valve, typically around 0.6 or 0.7.

Table 1 States of valves at each segment of $\Gamma(v)$

Γ	v	U	hR	hSC	pR	rSC	rR
$-F_{rM}$	+	$\mathcal{U}_+ \cup \mathcal{U}_0 \cup \mathcal{U}_-$	x	o	—	x	o
Γ_{+3}	+	$\mathcal{U}_+$	x	o	—	x	x
Γ_{+2b}	+	$\mathcal{U}_+$	x	x	o	x	o
Γ_{+2a}	+	$\mathcal{U}_+$	x	x	o	x	x
Γ_{+1b}	+	$\mathcal{U}_+$	x	x	x	x	o
Γ_{+1a}	+	$\mathcal{U}_+$	x	x	x	x	x
Γ_{+0b}	+	$\mathcal{U}_+$	o	x	—	x	o
Γ_{+0a}	+	$\mathcal{U}_+$	o	x	—	x	x
$[\Gamma_+(0), F_{hM}]$	0	$\mathcal{U}_+$	x	x	—	x	x
$[-F_{rM}, F_{hM}]$	0	$\mathcal{U}_0$	x	x	—	x	x
$[-F_{rM}, \Gamma_-(0)]$	0	$\mathcal{U}_-$	x	x	—	x	x
Γ_{-0a}	−	$\mathcal{U}_-$	x	x	—	x	o
Γ_{-0b}	−	$\mathcal{U}_-$	o	x	—	x	o
Γ_{-1a}	−	$\mathcal{U}_-$	x	x	x	x	x
Γ_{-1b}	−	$\mathcal{U}_-$	o	x	x	x	x
Γ_{-2a}	−	$\mathcal{U}_-$	x	x	o	x	x
Γ_{-2b}	−	$\mathcal{U}_-$	o	x	o	x	x
Γ_{-3}	−	$\mathcal{U}_-$	x	x	—	o	x
F_{hM}	−	$\mathcal{U}_+ \cup \mathcal{U}_0 \cup \mathcal{U}_-$	o	x	—	o	x

hR = head-side relief valve; hSC = head-side suction check valve; pR = pump relief valve; rSC = rod-side suction check valve; rR = rod-side relief valve; o = open; x = closed; and - = either open or closed.

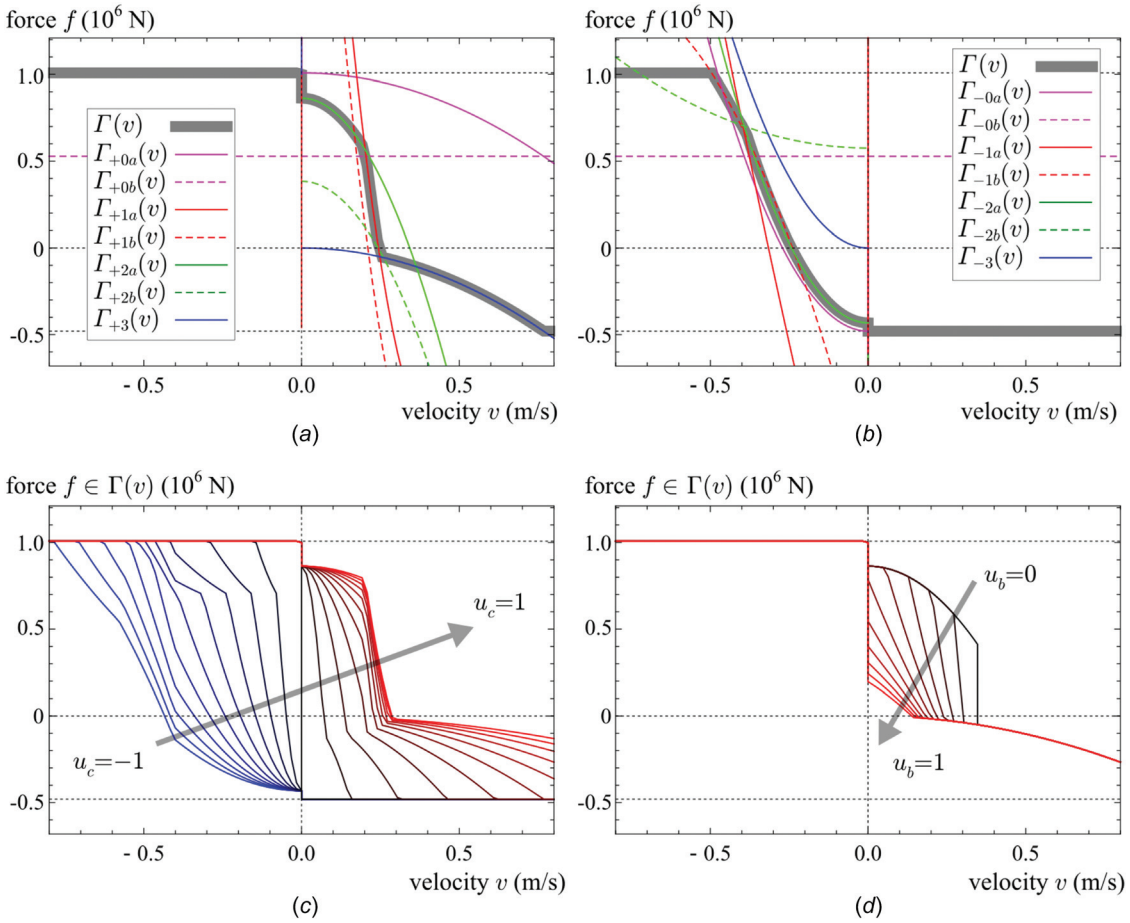

Fig. 3 Numerical examples of the quasi-static map $f \in \Gamma(v)$. (*a*) $u_c = 0.5$, $u_b = 0.2$; (*b*) $u_c = -0.5$, $u_b = 0.2$; (*c*) $u_c \in [-1, 1]$, $u_b = 0.2$; and (*d*) $u_c = 0.7$, $u_b \in [0, 1]$. The force f is positive when the external force is compressive and the actuator force acts to extend the rod.

With this regeneration pipeline and its flowrate Q_a, Eq. (21) is extended into the following:

$$-v + \widehat{u}_{ph}\mathcal{R}(A_h P_c - F_h) - \widehat{u}_{th}\mathcal{R}(F_h) \in \mathcal{N}_{[0,F_{hM}]}(F_h) - Q_a/A_h \tag{36a}$$

$$v + \widehat{u}_{pr}\mathcal{R}(A_r P_c - F_r) - \widehat{u}_{tr}\mathcal{R}(F_r) \in \mathcal{N}_{[0,F_{rM}]}(F_r) + Q_a/A_r \tag{36b}$$

$$A_h\widehat{u}_{ph}\mathcal{R}(A_h P_c - F_h) + A_r\widehat{u}_{pr}\mathcal{R}(A_r P_c - F_r) \in \mathcal{N}_{(-\infty,P_c]}(P) \tag{36c}$$

$$\begin{aligned} Q \in U_b\mathcal{R}(P) + A_h\widehat{u}_{ph}\mathcal{R}(A_h P_c - F_h) \\ + A_r\widehat{u}_{pr}\mathcal{R}(A_r P_c - F_r) + \mathcal{N}_{(-\infty,P_M]}(P) \end{aligned} \tag{36d}$$

$$f = F_h - F_r \tag{36e}$$

With $Q_a = 0$, which results from $u_a = 0$, Eq. (36) reduces to Eq. (21). Let us assume that u_a is set positive only when $\widehat{\boldsymbol{u}} \in \mathcal{U}_+$ because it is the case in many practical hydraulic circuits. In addition, we assume that $u_{tr} > 0$ for the simplicity. Under these conditions, Eqs. (35) and (36) reduce to the following:

$$\widehat{A}v_a - v + \widehat{u}_{ph}\mathcal{R}(A_h P_c - F_h) \in \mathcal{N}_{[0,F_{hM}]}(F_h) \tag{37a}$$

$$v - v_a - \widehat{u}_{tr}\mathcal{R}(F_r) \in \mathcal{N}_{[0,F_{rM}]}(F_r) \tag{37b}$$

$$A_h\widehat{u}_{ph}\mathcal{R}(A_h P_c - F_h) \in \mathcal{N}_{(-\infty,P_c]}(P) \tag{37c}$$

$$Q \in U_b\mathcal{R}(P) + A_h\widehat{u}_{ph}\mathcal{R}(A_h P_c - F_h) + \mathcal{N}_{(-\infty,P_M]}(P) \tag{37d}$$

$$f = F_h - F_r \tag{37e}$$

$$v_a = \widehat{u}_a \max\left(\mathcal{R}\left(F_r - \widehat{A}F_h, 0\right)\right) \tag{37f}$$

where $v_a \triangleq Q_a/A_r$, $\widehat{u}_a \triangleq c_a u_a / A_r^{3/2}$, and $\widehat{A} = A_r/A_h$.

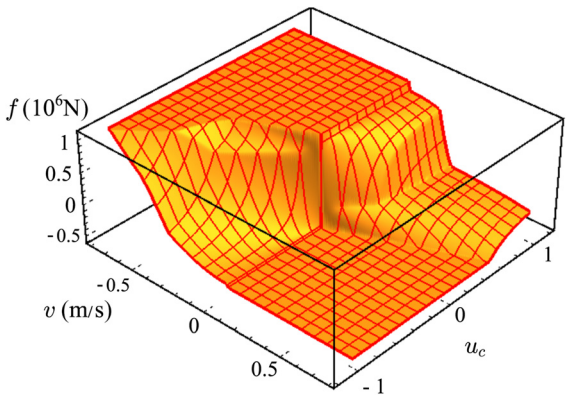

Fig. 4 Numerical examples of the quasi-static map $f \in \Gamma(v)$ with varying u_c and the fixed $u_b = 0.2$. The force f is positive when the external force is compressive and the actuator force acts to extend the rod.

By carefully observing Eq. (37), one can see that $v_a > 0$ implies $F_r > 0$ from Eq. (37*f*), which implies $v_a \le v$ from Eq. (37*b*). Its contraposition is that $v_a > v$ implies $v_a = 0$. Therefore, Eq. (37) imposes the condition $0 \le v_a \le \max(0, v)$. When $v < 0$, the solutions are obviously $v_a = 0$ and $f \in \Gamma(v)$. Therefore, hereafter we consider only the case $v > 0$, in which $v_a > 0$ may take place. By using the functions defined in Eqs. (28*a*) and (28*b*), the first four equations of Eq. (37) can be rewritten as $F_h \in \Gamma_h\left(v - \widehat{A} v_a\right)$ and $F_r \in \Gamma_r(v - v_a)$ with P_c and P being eliminated. Considering the definitions of Γ_h and Γ_r, because of the conditions $v - v_a \ge 0$, $v > 0$, $u_{tr} > 0$, and $\widehat{A} \in (0, 1)$, Γ_h and Γ_r are always single-valued and thus can be replaced by Γ_{h+} and Γ_{r+}, respectively. Therefore, Eq. (37) can be rewritten as follows:

$$\Xi_v(v, v_a) \in -\mathcal{N}_{[0,\infty)}(v_a) \tag{38a}$$

$$f = \Gamma_{h+}\left(v - \widehat{A} v_a\right) - \Gamma_{r+}(v - v_a) \tag{38b}$$

where

$$\Xi_v(v, v_a) \triangleq S(v_a) - \widehat{u}_a^2\left(\Gamma_{r+}(v - v_a) - \widehat{A}\Gamma_{h+}\left(v - \widehat{A} v_a\right)\right) \tag{39}$$

This expression can be seen as an algebraic problem regarding $\{f, v_a\}$ with a given v.

The function $\Xi_v(v, v_a)$ is an increasing function of v_a and it satisfies $\Xi_v(v, v) > 0$ because of $\Gamma_{r+}(0) = 0$. With the algebraic constraint (38*a*), $\Xi_v(v, 0) \ge 0$ implies that the solution is $v_a = 0$, Meanwhile, if $\Xi_v(v, 0) < 0$, the solution can be found within the region $v_a \in [0, v]$ by simple root-finding schemes. Once the solution v_a is obtained, f is obtained by Eq. (38*b*).

In conclusions, f and v_a satisfying Eq. (38) are obtained by the following functions:

$$f \in \Gamma_{\mathrm{reg}}\left(v\right) \triangleq \begin{cases} \Gamma(v) \text{if } u_a = 0 \vee \widehat{\boldsymbol{u}} \notin \mathcal{U}_+ \vee v \le 0 \vee \Xi_v(v, 0) \ge 0 \\ \Gamma_{h+}\left(v - \widehat{A}\widehat{v}_a(v)\right) - \Gamma_{r+}\left(v - \widehat{v}_a(v)\right) \text{otherwise} \end{cases} \tag{40}$$

$$v_a = \widehat{v}_a\left(v\right) \triangleq \begin{cases} 0 \text{if} u_a = 0 \vee \widehat{\boldsymbol{u}} \notin \mathcal{U}_+ \vee v \le 0 \vee \Xi_v(v, 0) \ge 0 \\ \mathrm{FindRoot}\left(\Xi_v(v, \bullet), [0, v]\right) \text{otherwise} \end{cases} \tag{41}$$

Here, "FindRoot" is a function that finds a root of the argument function within the range specified by the second argument. This computation can be performed with a common iterative method, such as the bisection method or the false position method, because $\Xi_v(v, v_a)$ is continuous and monotonic. It may also be possible to find analytical methods because $\Xi_v(v, v_a)$ is only a piecewise parabolic function. The function Γ_{reg} can be seen as an extension of the quasi-static map Γ given in Sec. 3.4.

Some numerical examples of Γ_{reg} and $\widehat{v}_a$ are presented in Fig. 6. It can be seen that, as u_a increases (i.e., as the regeneration valve opens), the extending velocity of the rod tends to increase especially in the region $f < 0$, i.e., under stretching external forces. It can also be seen that the flowrate Q_a through the regeneration valve increases as u_a and v increase. These features are consistent with those of actual hydraulic actuators.

5 Extension 2: Multiple Actuators Driven by One Pump

In some excavators, more than one actuator is actuated by a single pump as illustrated in Fig. 7. In such a circuit, the behaviors of the actuators influence each other, e.g., the movement of one actuator may decrease the supplied flowrate to other actuators. This

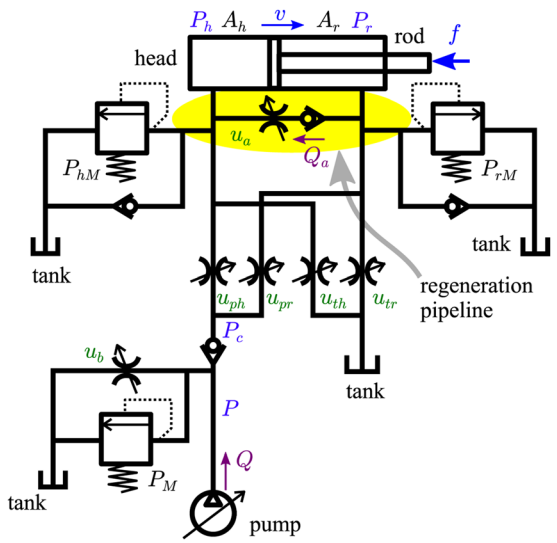

Fig. 5 Regeneration pipeline added to the circuit of Fig. 1

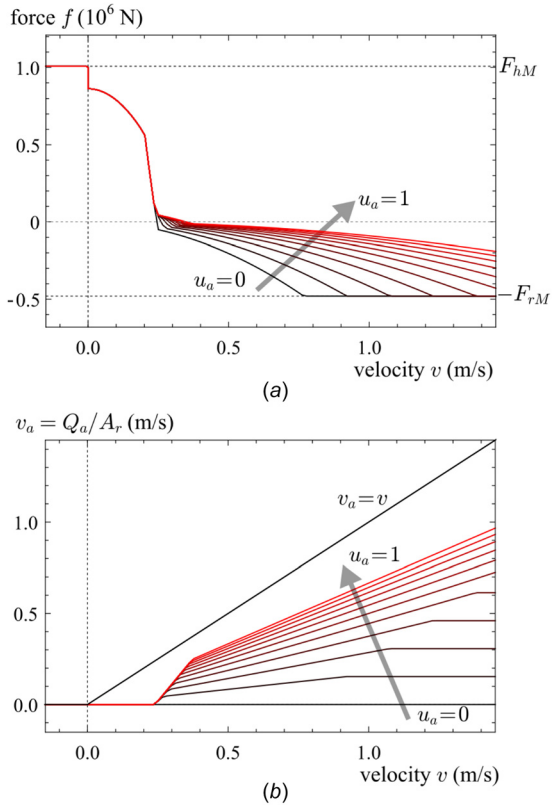

Fig. 6 Numerical examples of the quasi-static map $f \in \Gamma_{\mathrm{reg}}(v)$ and $v_a = \widehat{v}_a(v)$ of the circuit of Fig. 5, which includes a regeneration pipeline. The parameters are set the same as in Sec. 3.5 except $C_a = 0.6$ and $a_a = 0.0001$ m^2. The valve openings are set as $u_c = 0.5$ (see Eq. (33)) and $u_b = 0.2$.

section presents an extension of the quasi-static model to deal with such systems.

In circuits like Fig. 7, the actuators are connected to a junction at which the pressure is P, and the total supplied flowrate Q from the pump is equal to the sum of the supplied flowrates to all actuators plus that discharged through the bleed valve and the pump relief valve. On the other hand, the actuator model developed in Sec. 3.4 assumes that the supplied flowrate Q from the pump is the input to be given. Therefore, one can see that it is convenient

to have a modified version of the quasi-static map Γ of which the input is the pressure P instead of the flowrate Q.

With a close look at the definition (30) of the function Γ in Sec. 3.4, one can see that a P-input version of the quasi-static map Γ can be obtained by replacing P_m by P and removing the segments depending on Q. Specifically, the modified version $\widehat{\Gamma}(P,v)$, which maps the velocity v to the force f of an actuator depending on P, can be given as follows:

$$f \in \widehat{\Gamma}(P,v) \triangleq \mathrm{gsgn}\Big(\widehat{\Gamma}_-(P,v), v, \widehat{\Gamma}_+(P,v)\Big) \tag{42a}$$

where

$$\widehat{\Gamma}_+(P,v) \triangleq \max(\min(\max(\Gamma_{+0a}(v), \Gamma_{+0b}(v)), \max(\widehat{\Gamma}_{+2a}(P,v), \widehat{\Gamma}_{+2b}(P,v))), \quad \Gamma_{+3}(v), -F_{hM}) \tag{42b}$$

$$\widehat{\Gamma}_-(P,v) \triangleq \min(\max(\min(\Gamma_{-0a}(v), \Gamma_{-0b}(v)), \min(\widehat{\Gamma}_{-2a}(P,v), \widehat{\Gamma}_{-2b}(P,v))), \quad \Gamma_{-3}(v), F_{hM}) \tag{42c}$$

$$\widehat{\Gamma}_{+2a}(P,v) \triangleq A_h P - \frac{\mathcal{S}(v)}{\widehat{u}_{ph}^2} - \frac{\mathcal{S}(v)}{\widehat{u}_{tr}^2} \tag{42d}$$

$$\widehat{\Gamma}_{+2b}(P,v) \triangleq A_h P - \frac{\mathcal{S}(v)}{\widehat{u}_{ph}^2} - F_{rM} \tag{42e}$$

$$\widehat{\Gamma}_{-2a}(P,v) \triangleq -A_r P - \frac{\mathcal{S}(v)}{\widehat{u}_{pr}^2} - \frac{\mathcal{S}(v)}{\widehat{u}_{th}^2} \tag{42f}$$

$$\widehat{\Gamma}_{-2b}(P,v) \triangleq -A_r P - \frac{\mathcal{S}(v)}{\widehat{u}_{pr}^2} + F_{hM} \tag{42g}$$

Here, the functions without hats are those defined in Eq. (30). In the same manner as Eq. (31), we also have the following:

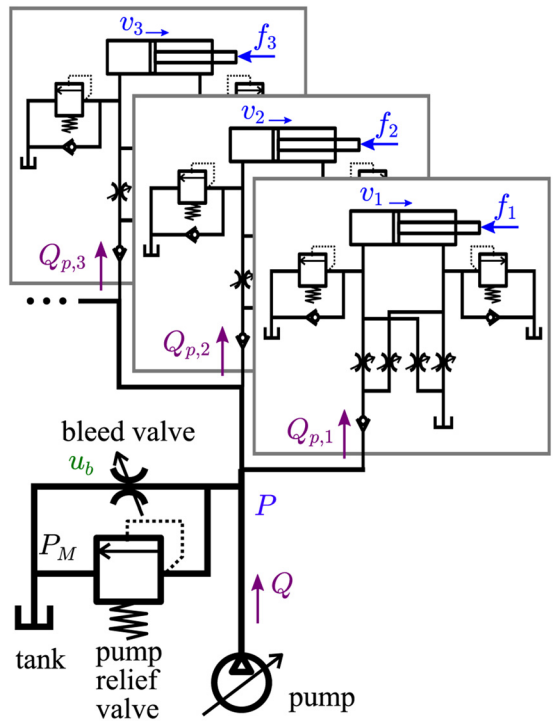

Fig. 7 Multiple actuators driven by one pump

$$\begin{aligned}\widehat{\Gamma}_+(P,0) &= \widehat{\Gamma}_{h+}(P,0) - \widehat{\Gamma}_{r+}(P,0)\\ \widehat{\Gamma}_-(P,0) &= \widehat{\Gamma}_{h-}(P,0) - \widehat{\Gamma}_{r-}(P,0)\end{aligned} \tag{43a}$$

where

$$\widehat{\Gamma}_{h+}(P,0) = \begin{cases} \min(F_{hM}, A_h P) & \text{if } \widehat{u}_{ph} > 0 \\ 0 & \text{if } \widehat{u}_{ph} = 0 \end{cases} \tag{43b}$$

$$\widehat{\Gamma}_{r+}(P,0) = \begin{cases} 0 & \text{if } \widehat{u}_{tr} > 0 \\ F_{rM} & \text{if } \widehat{u}_{tr} = 0 \end{cases} \tag{43c}$$

$$\widehat{\Gamma}_{h-}(P,0) = \begin{cases} 0 & \text{if } \widehat{u}_{th} > 0 \\ F_{hM} & \text{if } \widehat{u}_{th} = 0 \end{cases} \tag{43d}$$

$$\widehat{\Gamma}_{r-}(P,0) = \begin{cases} \min(F_{rM}, A_r P_M) & \text{if } \widehat{u}_{pr} > 0 \\ 0 & \text{if } \widehat{u}_{pr} = 0 \end{cases} \tag{43e}$$

The flowrate Q_p into an actuator is determined by the pressure P at the junction and the pressure P_h or P_r of the chamber connected to the pump, specifically, as follows:

$$\begin{aligned}Q_p = {} & A_h \widehat{u}_{ph} \max(\mathcal{R}(A_h P - F_h), 0) \\ & + A_r \widehat{u}_{pr} \max(\mathcal{R}(A_r P - F_r), 0)\end{aligned} \tag{44}$$

If $\widehat{\boldsymbol{u}} \in \mathcal{U}_+$, we have $F_h = f + F_r$ and $F_r = \mathrm{proj}_{[0,F_{rM}]}\Big(\mathcal{S}(v)/\widehat{u}_{tr}^2\Big)$. If $\widehat{\boldsymbol{u}} \in \mathcal{U}_-$, we have $F_h = \mathrm{proj}_{[0,F_{hM}]}\Big(\mathcal{S}(v)/\widehat{u}_{th}^2\Big)$ and $F_r = F_h - f$. Therefore, Q_p is obtained as follows:

$$Q_p = \widehat{Q}_p\Big(P, v, \widehat{\Gamma}(P,v)\Big) \tag{45}$$

where

$$\widehat{Q}_p(P,v,f) \triangleq \begin{cases} A_h \widehat{u}_{ph} \max\Big(\mathcal{R}\Big(A_h P - \mathrm{proj}_{[0,F_{rM}]}\Big(\mathcal{S}(v)/\widehat{u}_{tr}^2\Big) - f\Big), 0\Big) \\ \qquad \text{if } \widehat{\boldsymbol{u}} \in \mathcal{U}_+ \\ 0 \qquad \text{if } \widehat{\boldsymbol{u}} \in \mathcal{U}_0 \\ A_r \widehat{u}_{pr} \max\Big(\mathcal{R}\Big(A_r P - \mathrm{proj}_{[0,F_{hM}]}\Big(-\mathcal{S}(v)/\widehat{u}_{th}^2\Big) + f\Big), 0\Big) \\ \qquad \text{if } \widehat{\boldsymbol{u}} \in \mathcal{U}_- \end{cases} \tag{46}$$

The function $\widehat{\Gamma}$ appearing in Eq. (45) may be set-valued at $v = 0$, but a careful observation of its limits of both sides of zero shows that $\widehat{Q}_p(P, 0, \widehat{\Gamma}(P,0)) = 0$, single-valued, under all three conditions, $\mathcal{U}_+$, $\mathcal{U}_0$, and $\mathcal{U}_-$.

By using the function $\widehat{Q}_p$, the algebraic constraint between the total flowrate Q from the pump and the pressure P can be described as follows:

$$\Xi_P(P) \in \mathcal{N}_{(-\infty,P_M]}(P) \tag{47a}$$

where

$$\Xi_P(P) \triangleq Q - U_b \mathcal{R}(P) - \sum_{j=1}^{N} \widehat{Q}_{p,j}\Big(P, v_j, \widehat{\Gamma}_j(P, v_j)\Big) \tag{47b}$$

Here, the symbols with the subscript j stand for those associated with the jth actuator, and N denotes the number of actuators. The value of $\Xi_P(P)$ can be interpreted as the flowrate from the pump relief valve (see Fig. 7), which is the difference between the oil

supply from the pump and the sum of the oil supplies to all actuators plus that to the bleed valve. As long as $P < P_M$, Eq. (47*a*) reduces to $\Xi_P(P) = 0$, which means that the pump relief valve is closed. When $P = P_M$, Eq. (47*a*) reduces to $\Xi_P(P) \geq 0$, which means that the oil is discharged from the pump relief valve, of which the pressure limit is P_M. The pressure P can be found by solving the algebraic problem (47) as follows:

$$P = \begin{cases} P_M & \text{if } \Xi_P(P_M) \geq 0 \\ \text{FindRoot}\left(\Xi_P(\bullet), [0, P_M]\right) & \text{otherwise} \end{cases} \tag{48}$$

This FindRoot is also easy because of the monotonicity of the function Ξ_P.

By using the value of P obtained by Eq. (48), the quasi-static relation between the forces $\boldsymbol{f} = [f_1, \ldots, f_N]^T$ and the velocities $\boldsymbol{v} = [v_1, \ldots, v_N]^T$ of N actuators is written in the following form:

$$\boldsymbol{f} \in \boldsymbol{\Gamma}_{\text{mul}}(\mathbf{v}) \triangleq \left[\widehat{\Gamma}_1(P, v_1), \ldots, \widehat{\Gamma}_N(P, v_N)\right]^T \tag{49}$$

where P is the one obtained by Eq. (48).

Some numerical examples are shown in Fig. 8. In these examples, two identical actuators 1 and 2 share a single pump. The parameters of the actuators are the same as those in Sec. 3.5. The force f_1 obtained by the map $[f_1, f_2]^T \in \boldsymbol{\Gamma}_{\text{mul}}\left([v_1, v_2]^T\right)$ according to the variable v_1 and some fixed values of v_2 are shown in Figs. 8(*a*) and 8(*d*). Intermediate values P and $\Xi_P(P)$, which are the immediate output of the root finding in Eq. (48), are presented in Figs. 8(*b*), 8(*c*), 8(*e*), and 8(*f*). It can be seen that an increased speed v_2 of the actuator 2 results in a decreased speed v_1 of the actuator 1, a decreased pressure P at the junction, and a decreased flowrate $\Xi_P(P)$ from the pump relief valve, which are consistent with what can happen in real hydraulic circuits. Note that this example uses two identical actuators only for simplicity. This approach can also be applied to circuits comprising different actuators or more than two actuators.

6 Conclusions

This paper has presented a nonsmooth representation of the quasi-static characteristics of a hydraulic actuator driven by a four-valve independent metering circuit, being motivated by those used in commercial excavators. It is described as a nonsmooth map between the velocity and the force. The representation is derived from the algebraic constraint between the flowrate and the pressure at every valve in the circuit in the steady-state. In addition, the presented approach is extended to include a regeneration pipeline and to deal with a collection of actuators driven by a single pump. This paper has shown that these complicated circuit structures are analytically tractable through an extension of the conventional hydraulic–electric analogy.

The presented approach has been illustrated through the visualization of the actuator's steady-state force–velocity relation with some sets of graphs. To obtain these graphs, one would need iterative computation if a dynamical model is used, but they are obtained as a closed-form analytical representation with the quasi-static model. The obtained force–velocity maps can be seen as potentially useful to grasp "nominal" characteristics of the actuators. Usually, grasping the steady-state characteristics can be a basis to grasp the whole characteristics including the dynamics. Future studies should address the extension of the model to include the pressure dynamics and the transient response, which may be realized by including some additional terms regarding the pressure derivative in the presented representation.

Because the presented model only deals with the steady-states, which is only an aspect of the whole physical characteristics of the actuator, its quantitative or empirical validation would not be very straightforward. Direct experimental validation of the model would require that the measurement of the force be performed while maintaining a constant velocity of the actuator for a certain period of time, but it might not always be possible. The validation would need to be performed on applications or extensions of the model, rather than on the model alone. For example, some quantitative validation would need to be performed on dynamical models that could be obtained as extensions of the presented

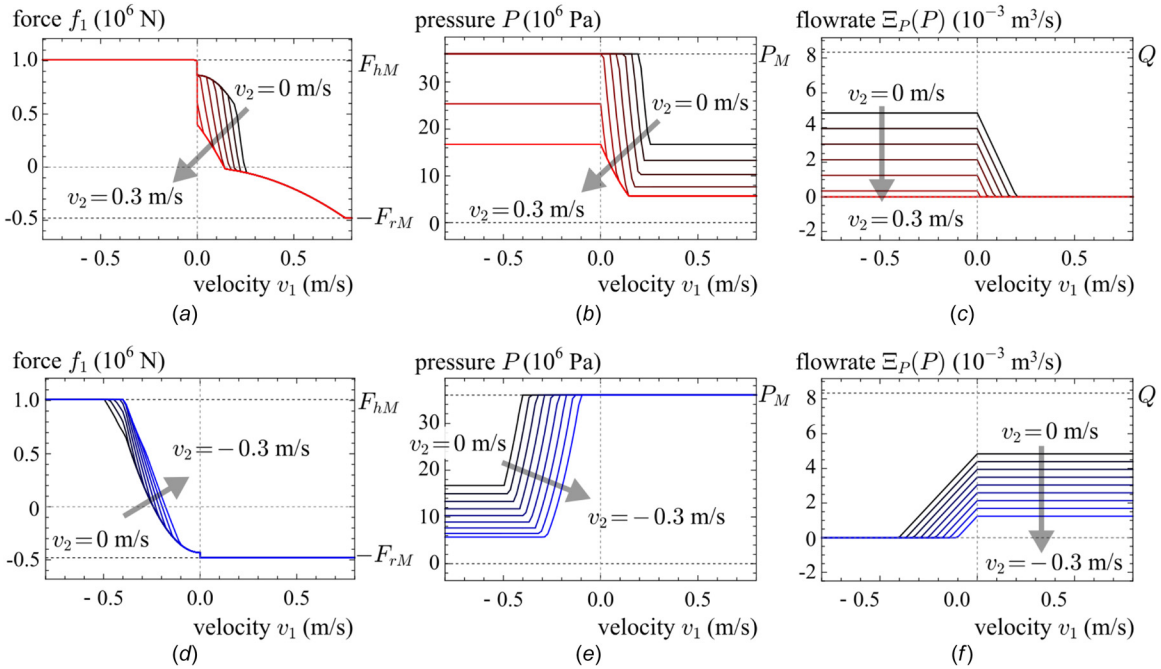

Fig. 8 Numerical examples regarding the quasi-static map $[f_1, f_2]^T \in \Gamma_{\text{mul}}([v_1, v_2]^T)$ of a circuit including two identical actuators driven by a single pump. Positive commands $u_{c,1} = u_{c,2} = 0.5$ (see Eq. (33)) and some different values of v_2 between 0 m/s and 0.3 m/s are given in (*a*)–(*c*). Negative commands $u_{c,1} = u_{c,2} = -0.5$ and some different values of v_2 between 0 m/s and −0.3 m/s are given in (*d*)–(*f*).

quasi-static model. It would also be the case with controllers built upon the proposed model, of which the control performance in terms of accuracy and robustness would need to be evaluated.

For the convenience of the computation, analytical methods should be sought for the root-finding routines that have appeared in the proposed algorithms in Secs. 4 and 5. Integration of the schemes of Secs. 4 and 5, i.e., multiple actuators with regeneration pipelines driven by a single pump, is also an open problem.

Funding Data

- Kobelco Construction Machinery Co., Ltd.

Appendix: Derivation From Eq. (25) to Eq. (26)

This appendix section presents the details of the derivation from Eq. (25) to Eq. (26) under the condition $\widehat{\boldsymbol{u}} \in \mathcal{U}_+$. First, one can rewrite Eqs. (25*a*)–(25*c*) as follows:

$$F_h = \mathrm{proj}_{[0,F_{hM}]}\left(A_h P_c - \mathcal{S}(v)/\widehat{u}_{ph}^2\right) \tag{A1a}$$

$$F_r = \mathrm{proj}_{[0,F_{rM}]}\left(\mathcal{S}(v)/\widehat{u}_{tr}^2\right) \tag{A1b}$$

$$P_c = \max(P, F_h/A_h) \tag{A1c}$$

respectively, because of Theorem 1. Now F_r is obtained as Eq. (A1*b*), which is Eq. (26*b*), and thus we hereafter attempt to obtain F_h from Eqs. (A1*a*), (A1*c*), and (25*d*). Substituting Eq. (A1*c*) into Eqs. (A1*a*) and (25*d*) results in the following:

$$F_h = \mathrm{proj}_{[0,F_{hM}]}\left(\max(A_h P, F_h) - \mathcal{S}(v)/\widehat{u}_{ph}^2\right) \tag{A2a}$$

$$Q \in U_b \mathcal{R}(P) + A_h \widehat{u}_{ph} \mathcal{R}(\max(A_h P - F_h, 0)) + \mathcal{N}_{(-\infty,P_M]}(P) \tag{A2b}$$

If $v < 0$, Eq. (A2*a*) implies that $F_h = F_{hM}$. If $v = 0$, Eq. (A2*a*) implies that $\min(A_h P, F_{hM}) \le F_h \le F_{hM}$. If $v = 0$ and $F_h < F_{hM}$, Eq. (A2*a*) implies $F_h \ge A_h P$ and substituting it into Eq. (A2*b*) yields $P = \min\left(P_M, Q^2/U_b^2\right)$. Therefore, if $v = 0$, the condition (A2) implies the following:

$$F_h \in \left[\min\left(F_{hM}, A_h P_M, A_h Q^2/U_b^2\right), F_{hM}\right] \tag{A3}$$

The case of $v > 0$ with Eq. (A2) needs some considerations. If $v > 0$, Eq. (A2*a*) implies $A_h P > F_h$ and thus Eq. (A2) can be rewritten as follows:

$$F_h = \mathrm{proj}_{[0,F_{hM}]}\left(A_h P - \mathcal{S}(v)/\widehat{u}_{ph}^2\right) \tag{A4a}$$

$$\begin{aligned} Q \in U_b \mathcal{R}(P) + A_h \widehat{u}_{ph} \mathcal{R}\big(A_h P - \mathrm{proj}_{[0,F_{hM}]} \\ \left(A_h P - \mathcal{S}(v)/\widehat{u}_{ph}^2\right)\big) + \mathcal{N}_{(-\infty,P_M]}(P) \end{aligned} \tag{A4b}$$

If $A_h P - \mathcal{S}(v)/\widehat{u}_{ph}^2 \in [0, F_{hM}]$, Eq. (A4*b*) can be rewritten as follows:

$$\begin{aligned} (53\mathrm{b}) &\iff Q \in U_b \mathcal{R}(P) + A_h \widehat{u}_{ph} \mathcal{R}\left(\mathcal{S}(v)/\widehat{u}_{ph}^2\right) \\ &\quad + \mathcal{N}_{(-\infty,P_M]}(P) \\ &\iff Q \in U_b \mathcal{R}(P) + A_h v + \mathcal{N}_{(-\infty,P_M]}(P) \\ &\iff P = \min\left(P_M, -\frac{A_h^2}{U_b^2}\mathcal{S}\left(v - \frac{Q}{A_h}\right)\right) \end{aligned} \tag{A5}$$

and substituting it into Eq. (A4*a*) results in the following:

$$F_h = \mathrm{proj}_{[0,F_{hM}]}\left(\min\left(A_h P_M, -\frac{A_h^3}{U_b^2}\mathcal{S}\left(v - \frac{Q}{A_h}\right)\right) - \frac{\mathcal{S}(v)}{\widehat{u}_{ph}^2}\right) \tag{A6}$$

This means that $A_h P - \mathcal{S}(v)/\widehat{u}_{ph}^2 \in [0, F_{hM}]$ reduces Eq. (A4) into Eqs. (A5) and (A6). Meanwhile, if $A_h P - \mathcal{S}(v)/\widehat{u}_{ph}^2 \le 0$, Eq. (A4*a*) results in $F_h = 0$. In the same light, if $A_h P - \mathcal{S}(v)/\widehat{u}_{ph}^2 \ge F_{hM}$, Eq. (A4*a*) results in $F_h = F_{hM}$ and it also reduces Eq. (A6) to $F_h = F_{hM}$. Therefore, if $v > 0$, Eq. (A2) leads to Eq. (A6) in any cases.

In conclusions, unifying the three cases, i.e., $F_h = F_{hM}$ for $v < 0$, Eq. (A3) for $v = 0$, and Eq. (A6) for $v > 0$, we have the expression (26*a*) for the case $\widehat{\boldsymbol{u}} \in \mathcal{U}_+$. Recalling that Eq. (26*b*) has already been obtained from Eq. (A1), one can see that Eq. (25) results in Eq. (26) in the case of $\widehat{\boldsymbol{u}} \in \mathcal{U}_+$.

References

[1] Akers, A., Gassman, M., and Smith, R., 2006, *Hydraulic Power System Analysis*, CRC Press, Boca Raton, FL.

[2] Gassman, M. P., 1993, "Use of the Hydraulic Ohm to Determine Flow Distribution," SAE Paper No. 932489.

[3] Greenslade, T. B., Jr., 2003, "The Hydraulic Analogy for Electric Current," Phys. Teach., **41**(8), pp. 464–466.

[4] Esposito, A., 1969, "A Simplified Method for AnalyzingHydraulic Circuits by Analogy," Mach. Des., **41**(24), pp. 173–177.

[5] Tabor, K. A., 2005, "A Novel Method of Controlling a Hydraulic Actuator With Four Valve Independent Metering Using Load Feedback," SAE Paper No. 2005-01-3639.

[6] Shenouda, A., 2006, "Quasi-Static Hydraulic Control Systems and Energy Savings Potential Using Independent Metering Four-Valve Assembly Configuration," Ph.D. thesis, Georgia Institute of Technology, Atlanta, GA.

[7] Shenouda, A., and Book, W., 2008, "Optimal Mode Switching for a Hydraulic Actuator Controlled With Four-Valve Independent Metering Configuration," Int. J. Fluid Power, **9**(1), pp. 35–43.

[8] Choi, K., Seo, J., Nam, Y., and Kim, K. U., 2015, "Energy-Saving in Excavators With Application of Independent Metering Valve," J. Mech. Sci. Technol., **29**(1), pp. 387–395.

[9] Kim, K., Kim, M., Kim, D., and Lee, D., 2019, "Modeling and Velocity-Field Control of Autonomous Excavator With Main Control Valve," Automatica, **104**, pp. 67–81.

[10] Chang, P. H., and Lee, S.-J., 2002, "A Straight-Line Motion Tracking Control of Hydraulic Excavator System," Mechatronics, **12**(1), pp. 119–138.

[11] Zhang, X., Qiao, S., Quan, L., and Ge, L., 2019, "Velocity and Position Hybrid Control for Excavator Boom Based on Independent Metering System," IEEE Access, **7**, pp. 71999–72011.

[12] Kim, J., Jin, M., Choi, W., and Lee, J., 2019, "Discrete Time Delay Control for Hydraulic Excavator Motion Control With Terminal Sliding Mode Control," Mechatronics, **60**, pp. 15–25.

[13] Yao, J., Jiao, Z., Ma, D., and Yan, L., 2014, "High-Accuracy Tracking Control of Hydraulic Rotary Actuators With Modeling Uncertainties," IEEE/ASME Trans. Mechatron., **19**(2), pp. 633–641.

[14] Cristofori, D., and Vacca, A., 2015, "Modeling Hydraulic Actuator Mechanical Dynamics From Pressure Measured at Control Valve Ports," Proc. Inst. Mech. Eng., Part I: J. Syst. Control Eng., **229**(6), pp. 541–558.

[15] Ruderman, M., 2017, "Full- and Reduced-Order Model of Hydraulic Cylinder for Motion Control," Proceedings of 43rd Annual Conference of IEEE Industrial Electronics Society, Beijing, China, Oct. 29, pp. 7275–7280.

[16] Destro, M. C., and De Negri, V. J., 2018, "Method for Combining Valves With Symmetric and Asymmetric Cylinders for Hydraulic Systems," Int. J. Fluid Power, **19**(3), pp. 126–139.

[17] Ylinen, A., Marjamäki, H., and Mäkinen, J., 2014, "A Hydraulic Cylinder Model for Multibody Simulations," Comput. Struct., **138**(1), pp. 67–72.

[18] Sakai, S., and Stramigioli, S., 2018, "Visualization of Hydraulic Cylinder Dynamics by a Structure Preserving Nondimensionalization," IEEE/ASME Trans. Mechatron., **23**(5), pp. 2196–2206.

[19] Acary, V., Bonnefon, O., and Brogliato, B., 2010, "Time-Stepping Numerical Simulation of Switched Circuits Within the Nonsmooth Dynamical Systems Approach," IEEE Trans. Comput.-Aided Des. Integr. Circuits Syst., **29**(7), pp. 1042–1055.

[20] Addi, K., Adly, S., Brogliato, B., and Goeleven, D., 2007, "A Method Using the Approach of Moreau and Panagiotopoulos for the Mathematical Formulation of Non-Regular Circuits in Electronics," Nonlinear Anal.: Hybrid Syst., **1**(1), pp. 30–43.

[21] Goeleven, D., 2008, "Existence and Uniqueness for a Linear Mixed Variational Inequality Arising in Electrical Circuits With Transistors," J. Optim. Theory Appl., **138**(3), pp. 397–406.
[22] Rahikainen, J., Kiani, M., Sopanen, J., Jalali, P., and Mikkola, A., 2018, "Computationally Efficient Approach for Simulation of Multibody and Hydraulic Dynamics," Mech. Mach. Theory, **130**, pp. 435–446.
[23] Wang, L., Book, W. J., and Huggins, J. D., 2012, "Application of Singular Perturbation Theory to Hydraulic Pump Controlled Systems," IEEE/ASME Trans. Mechatron., **17**(2), pp. 251–259.
[24] Kiani Oshtorjani, M., Mikkola, A., and Jalali, P., 2019, "Numerical Treatment of Singularity in Hydraulic Circuits Using Singular Perturbation Theory," IEEE/ASME Trans. Mechatron., **24**(1), pp. 144–153.
[25] Hannaford, B., and Winters, J., 1990, "Actuator Properties and Movement Control: Biological and Technological Models," *Multiple Muscle Systems: Biomechanics and Movement Organization*, J. M. Winters, and S. L.-Y. Woo, eds., Springer, New York, pp. 101–196.
[26] Tondu, B., 2015, "What is an Artificial Muscle? A Systemic Approach," Actuators, **4**(4), pp. 336–352.
[27] Brogliato, B., Daniilidis, A., Lemaréchal, C., and Acary, V., 2006, "On the Equivalence Between Complementarity Systems, Projected Systems and Differential Inclusions," Syst. Control Lett., **55**(1), pp. 45–51.
[28] Acary, V., and Brogliato, B., 2008, *Numerical Methods for Nonsmooth Dynamical Systems: Applications in Mechanics and Electronics* (Lecture Notes in Applied and Computational Mechanics, Vol. 35), Springer, Berlin.
[29] Bauschke, H. H., and Combettes, P. L., 2016, *Convex Analysis and Monotone Operator Theory in Hilbert Spaces*, 2nd ed., Springer, Berlin.
[30] Eriksson, B., and Palmberg, J.-O., 2011, "Individual Metering Fluid Power Systems: Challenges and Opportunities," Proc. Inst. Mech. Eng., Part I: J. Syst. Control Eng., **225**(2), pp. 196–211.
[31] Borutzky, W., Barnard, B., and Thoma, J., 2002, "An Orifice Flow Model for Laminar and Turbulent Conditions," Simul. Modell. Pract. Theory, **10**(3–4), pp. 141–152.
[32] Lichtarowicz, A., Duggins, R. K., and Markland, E., 1965, "Discharge Coefficients for Incompressible Non-Cavitating Flow Through Long Orifices," J. Mech. Eng. Sci., **7**(2), pp. 210–219.
[33] Ye, Y., Yin, C.-B., Li, X.-D., Zhou, W.-J., and Yuan, F.-F., 2014, "Effects of Groove Shape of Notch on the Flow Characteristics of Spool Valve," Energy Convers. Manage., **86**, pp. 1091–1101.
[34] Wu, D., Burton, R., and Schoenau, G., 2002, "An Empirical Discharge Coefficient Model for Orifice Flow," Int. J. Fluid Power, **3**(3), pp. 13–19.